23rd ABCM International Congress of Mechanical Engineering
December 6-11, 2015, Rio de Janeiro, RJ, Brazil

NUMERICAL VALIDATION OF THE INVARIANT DESCRIPTOR OF CONJUGATE FORCED CONVECTION-CONDUCTION COOLING OF 3D PROTRUDING HEATERS IN CHANNEL FLOW

Murilo A. Barbur[1]
Paulo H. Dias dos Santos[2]
Thiago Antonini Alves[1]
Federal University of Technology – Paraná (UTFPR), [1]Ponta Grossa, [2]Curitiba, PR, Brazil
murilo_barbur@hotmail.com, psantos@utfpr.edu.br, thiagoaalves@utfpr.edu.br

Abstract. *In this work, 3D protruding heaters mounted on a conductive substrate in a horizontal rectangular channel with laminar airflow had their temperatures related to the independent power dissipation in each heater by means of a matrix G^+ with invariant coefficients. These coefficients are dimensionless and they were called the conjugate influence coefficients (g^+) due to the forced convection-conduction nature of the heaters' cooling process. The temperature increase for each heater in the channel was quantified so that the contributions due to self-heating and due to the power dissipation in the other heaters (both upstream and downstream) were clearly identified. For fixed geometry, fluid and flow rate, substrate and heater conductivities, the conjugate coefficients are invariant with the heat generation rate in the heaters' array. Some examples were shown, indicating the effects of the substrate thermal conductivity and the Reynolds number on a coefficient. The results were numerically obtained considering three 3D protruding heaters on a two-dimensional array, using the ANSYS/Fluent™ 15.0 software.*

Keywords: *thermal management, conjugate heat transfer, forced convection, conduction, invariant descriptor, conjugate influence coefficients*

1. INTRODUCTION

Moffat (1998) showed that for an array of heated blocks in channel flow, the coefficient h_m based on the mean flow temperature (T_m) just upstream of each block is invariant with the power level only if the power dissipation is uniform in all the blocks. Otherwise, the resulting h_m and the corresponding *Nusselt* number are distinct for each heating condition. Arvizu & Moffat (1982) proposed the adiabatic surface temperature (T_{ad}) of each block as the reference, giving rise to the adiabatic heat transfer coefficient (h_{ad}), defined by

$$h_{ad} = \frac{q_{cv}/A_h}{\left(T_h - T_{ad}\right)} \tag{1}$$

This concept was subsequently developed by Moffat & Anderson (1990), Anderson & Moffat (1992a, 1992b), and Moffat (2004). The adiabatic temperature had been used by Eckert & Drake (1972) in the analysis of film cooling and heat transfer at high velocities – but Moffat and co-workers further developed the concept and applied it to electronics cooling. They showed that this coefficient may be obtained from tests with a single heated element of the array at a time and that it will be the same for any thermal boundary conditions of the array (for the same geometry, fluid and *Reynolds* number). This procedure may be applied to the forced convection cooling of the 1D array with three 2D heaters mounted on the substrate of a horizontal parallel plates channel. Considering an adiabatic substrate, the temperature rise of the n^{th} heater may be described as the sum of its adiabatic temperature rise and the rise due to self-heating, as follows

$$\left(T_h - T_0\right)_n = \left(T_{ad} - T_0\right)_n + \left(T_h - T_{ad}\right)_n \tag{2}$$

The first term on the right side of Eq. (2) is due to the heaters located upstream of the n^{th} heater (assuming parabolic behavior), while the second term is due to self-heating. Since the energy equation is linear, both terms may be expressed by means of a discrete superposition kernel function g^* proposed by Anderson & Moffat (1992a, 1992b), as follows

$$\left(T_h - T_0\right)_n = \sum_{i=1}^{n-1} \frac{q'_i}{\dot{m}' c_p} g^*_{ni} + \frac{q'_n}{\dot{m}' c_p} g^*_{nn} \tag{3}$$

In Eq. (3), q'_i is the heat released per unit depth from the i^{th} heater of the array, located upstream of the n^{th} heater and $\dot{m}'$ is the parallel plates channel mass flow rate per unit depth. The dimensionless kernel function $g_{ni}{}^*$ relates the n^{th}

heater adiabatic temperature rise to the q_i' release by the upstream i^{th} heater in the channel. It may be associated to the corresponding mean flow temperature rise as

$$g_{ni}^{*} = \frac{\left(T_{ad} - T_0 \right)_{ni}}{\left(\Delta T_m \right)_i} \tag{4}$$

The numerator on the right side of Eq. (4) is the adiabatic temperature rise of the n^{th} heater due to heat release at the i^{th} heater. The denominator represents the mean flow temperature rise due to the q_i' release at the i^{th} heater. Since the discrete heaters are mounted just on one plate of the channel, the flow temperature distribution is not uniform due to incomplete mixing and the kernel function g_{ni}^{*} is always greater than one.

The second kernel function in Eq. (3), g_{nn}^{*} represents the n^{th} heater temperature rise due to self-heating. It may also be expressed as the ratio of two temperature rises,

$$g_{nn}^{*} = \frac{\left(T_h - T_{ad} \right)_n}{\left(\Delta T_m \right)_n} \tag{5}$$

In Eq. (5), the numerator is the n^{th} heater temperature rise due to self-heating and the denominator is the corresponding mean flow temperature rise.

There are several investigations reported in the literature concerning the evaluation of the adiabatic heat transfer coefficient and the superposition kernel function g^{*} in channels with discrete heaters on an adiabatic surface (Alves & Altemani, 2012).

The concept of the discrete superposition kernel function was extended by Hacker and Eaton (1997) using an inverse discrete Green's function. Considering a 1D array of N heaters mounted on an adiabatic substrate, they expressed the temperature increase of the n^{th} heater by

$$\left(T_h - T_0 \right)_n = \sum_{i=1}^{N} g_{ni}^{-1} \, q_i \tag{6}$$

In Eq. (6), g_{ni}^{-1}, with units of [K/W], relates the convective heat release q_i at the i^{th} heater to the n^{th} heater average temperature rise. Both Eq. (6) and Eq. (3) are based on the superposition method due to the linearity of the energy equation (assuming forced convection and constant properties). The complete inverse Green's function with terms g_{ni}^{-1} may be expressed by a square matrix G^{-1} of order N as follows

$$\begin{bmatrix} \Delta T_1 \\ \Delta T_2 \\ \vdots \\ \Delta T_N \end{bmatrix} = \begin{bmatrix} g_{11}^{-1} & g_{12}^{-1} & \cdots & g_{1N}^{-1} \\ g_{21}^{-1} & g_{22}^{-1} & \cdots & g_{2N}^{-1} \\ \vdots & \vdots & \ddots & \vdots \\ g_{N1}^{-1} & g_{N2}^{-1} & \cdots & g_{NN}^{-1} \end{bmatrix} \begin{bmatrix} q_1 \\ q_2 \\ \vdots \\ q_N \end{bmatrix} \tag{7}$$

The heat release q_i from the heaters array is arbitrary, but the coefficients of the G^{-1} matrix are invariant descriptors of the process. This function may replace the adiabatic heat transfer coefficient as an invariant descriptor of the convective heat transfer (Alves & Altemani, 2012).

Considering now a conductive substrate, the heated blocks will be cooled by the conjugate forced convection-conduction mechanism. This problem may be solved numerically either considering a single coupled solid-fluid domain (Davalath & Bayazitoglu, 1987) or employing a decoupled procedure involving alternate separate solutions of the solid and the fluid regions (Anderson, 1994). The coupled solution of the conjugate problem is however the preferable method, on the grounds of a better accuracy and the always increasing availability of computers' memory and velocity.

The coupled technique was adopted in the work of Alves & Altemani (2012) for conjugate forced convection-conduction cooling of three 2D heaters mounted on a conductive substrate. Based on the linearity of the energy equation and on the principle of superposition, the temperature increase of each heater was expressed by

$$\left(T_h - T_0 \right)_n = \frac{1}{\dot{m}' c_p} \sum_{i=1}^{N} g_{ni}^{+} \, q'_i \tag{8}$$

or, in matrix form,

$$\begin{bmatrix} \Delta T_1 \\ \Delta T_2 \\ \vdots \\ \Delta T_N \end{bmatrix} = \frac{1}{\dot{m}' c_p} \begin{bmatrix} g_{11}^{+} & g_{12}^{+} & \cdots & g_{1N}^{+} \\ g_{21}^{+} & g_{22}^{+} & \cdots & g_{2N}^{+} \\ \vdots & \vdots & \ddots & \vdots \\ g_{N1}^{+} & g_{N2}^{+} & \cdots & g_{NN}^{+} \end{bmatrix} \begin{bmatrix} q_1 \\ q_2 \\ \vdots \\ q_N \end{bmatrix} \tag{9}$$

The n^{th} heater temperature ($T_{h,n}$) on the left side of Eq. (8) represents its average value at the interface with the airflow, evaluated from the numerical results. The terms g_{ni}^+ were called the conjugate influence coefficients and they are dimensionless, as the kernel function g_{ni}^* proposed by Anderson & Moffat (1992a, 1992b). For the same geometry, fluid and solid properties and *Reynolds* number, the conjugate coefficients are invariant with the heat generation rate in the heaters' array. The complete set of the coefficients g_{ni}^+ may be represented by a matrix G^+ – Eq. (9). Due to conduction in the substrate plate, the power dissipation in any heater influences the temperatures of all the other heaters of the array. Moreover, the flow recirculation between the protruding heaters also promotes upstream convection in the region between the heaters. These effects are included in the conjugate influence coefficients g_{ni}^+ defined by Eq. (8).

The coefficients g_{ni}^+ may be obtained most simply in forced convection from tests with a single heated element of the array at a time. Once all coefficients g_{ni}^+ were obtained, they were employed in Eq. (9) to predict the heaters temperatures under arbitrary power dissipation in the heaters array. These results were compared to those obtained directly from numerical simulations considering the same arbitrary power distribution in the array.

In this present work, the concept of the conjugate influence coefficients for 2D protruding heaters on a 1D array was numerically validated for conjugate forced convection-conduction cooling of the 2D array with 3D protruding heaters mounted on a conductive substrate. These results are important for the thermal design of electronic components assembled on circuit boards cooled by forced convection.

2. MODEL DESCRIPTION

The basic configuration consisted of a horizontal rectangular channel with three 3D protruding heaters mounted with perfect thermal contact on the lower wall, as indicated in Fig. 1. The channel geometry, including the conductive substrate and the heaters sizes and positions are indicated in this figure relative to the channel height (H), which was considered equal to 0.01 m in the numerical simulations. The fluid was always air and its properties were assumed at 27°C [~300 K] (Bergman *et al.*, 2012).

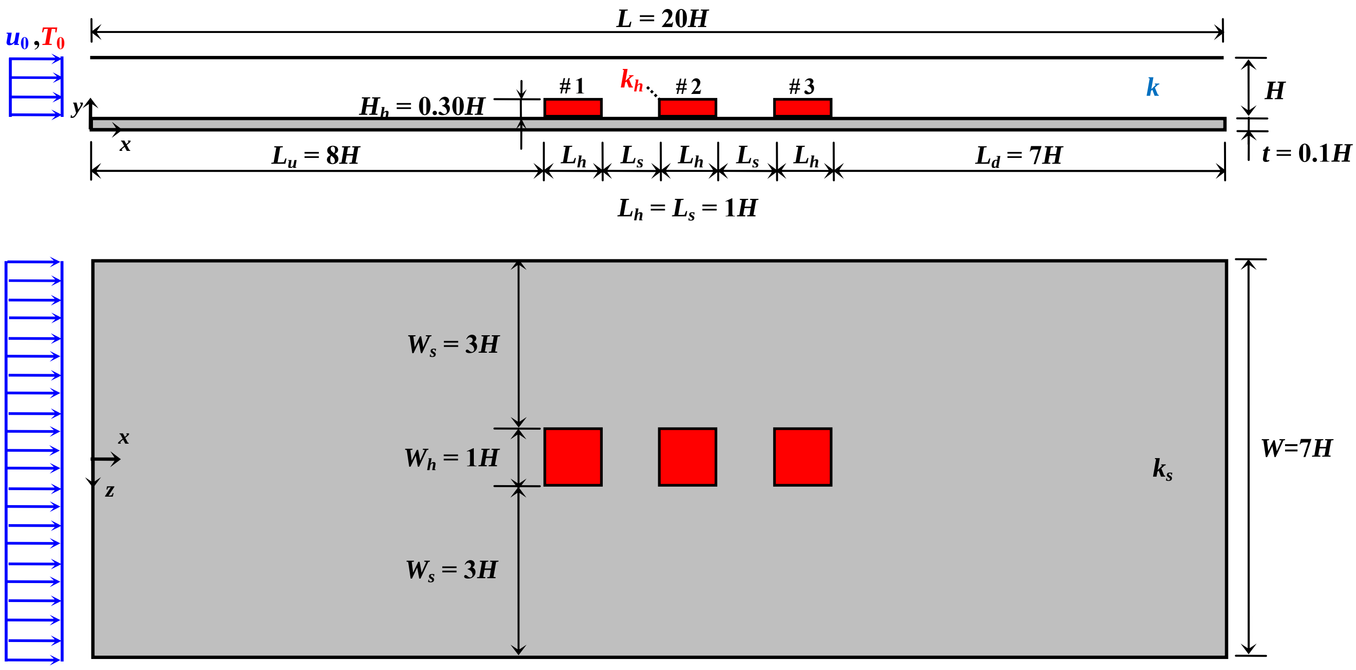

Figure 1. Basic configuration used for the tests

The domain upper and lower boundaries were impermeable and adiabatic as well as tips of the substrate plate, and at the channel inlet a steady air flow was forced in the laminar regime with uniform velocity (u_0) and temperature (T_0). The active heaters were considered with uniform volumetric heat generation rate. Due to the conductive substrate adiabatic lower surface, the heat conducted from a heater to the substrate plate eventually returned to the airflow by convection both upstream and downstream of the heater. A *Reynolds* number (Re) was defined with the 3D protruding heater height (H_h) and the uniform inlet velocity (u_0). Five values of Re were considered in the range from 100 to 300, corresponding to u_0 in the range from 0.5 m/s to 1.5 m/s. The substrate thermal conductivity (k_s) relative to the air (k) was investigated in the range of (k_s/k) from 0 (adiabatic substrate) to 84 (printed circuit board – Bar-Cohen *et al.*, 2003). The heaters thermal conductivity (k_h) relative to the air (k_h/k) was always to ≈ 10^4 (pure aluminum), so that the heaters were almost isothermal. The heaters height (H_h/H) was equal to 0.30 to avoid that flow recirculation downstream of the third heater extended beyond the channel end.

The domain indicated by Fig. 1, comprising the solid and fluid regions, was subdivided into non-superposing small control volumes which occupied a single solid or fluid region. The conservation equations of mass, *momentum*, and energy were then imposed in each control volume of the domain. On account of the problem symmetries, the conservation equations were formulated for the domain with length, L, width, $W/2$, and height, $(H + t)$. Natural convection effects were considered negligible in the present work, a procedure adopted in similar investigations (e.g., Alves & Altemani, 2012 and Zeng & Vafai, 2009). Considering steady state conditions and uniform properties in each control volume, the conservation equations were stated respectively as follows

$$\nabla \cdot \vec{u} = 0 \tag{10}$$

$$\rho\left(\vec{u} \cdot \nabla\right)\vec{u} = -\nabla p + \mu \nabla^2 \vec{u} \tag{11}$$

$$\rho c_p \left(\vec{u} \cdot \nabla\right) T = k \nabla^2 T + \delta S \tag{12}$$

In the energy equation, $\delta = 1$ in the 3D protruding heaters region and $\delta = 0$ in the substrate and the fluid regions. At the flow outlet, a negligible diffusion was assumed for the velocity components and the temperature.

A convective heat transfer coefficient for each heater was based on its average surface temperature at the interface with the airflow. The reference temperature was the flow inlet temperature (T_0). The 3D protruding heater length (L_h) was selected to define the average *Nusselt* number, as follows

$$\overline{Nu}_{0,n} = \frac{\overline{h}_{0,n} L_h}{k} = \frac{q'_{cv,n} \, L_h}{A_{cv}\left(T_h - T_0\right)_n k} \tag{13}$$

2.1 Numerical solution

The governing equations and their boundary conditions were numerically solved utilizing the Control Volume Method (Patankar, 1980) through the *ANSYS/Fluent*™ 15.0 software. The pressure-velocity coupling of the continuity and *momentum* equations, Eqs. (10-11), was treated via the *SIMPLE* algorithm. The convective-diffusive terms were discretized by the Second-Order Upwind Scheme. At the solid-fluid interfaces, use was made of the harmonic mean for the evaluation of the diffusion coefficients at the neighboring control volumes in order to handle the abrupt changes of the solid and fluid properties. The numerical procedures assumed were verified through a comparison with the numerical results of the thermo-fluid-dynamic parameters presented by ANSYS (2011). To obtain the numerical results, several numerical grids were tested before the final grid distribution was selected. The final grid was 3D non-uniform comprising 180,343 control volumes – Fig. 2. Additional tests showed that further grid refinement would not noticeably change the results. The iterative solution procedure for a typical case considering a conductive substrate took about 15 minutes in a microcomputer.

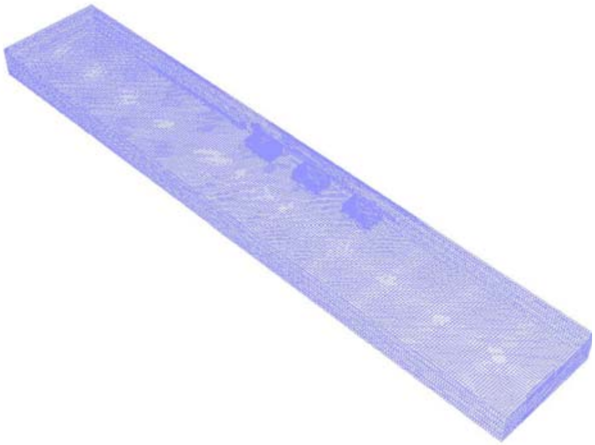

Figure 2. 3D non-uniform mesh (3D perspective view)

3. RESULTS AND DISCUSSION

3.1 Laminar airflow

In Fig. 3, the velocity profile of the air around an array of 3D protruding heaters is presented for $Re = 100$. The main characteristics of the laminar flow are the horseshoe vortices which start upstream the Heater #1 and develop around the heater's lateral surfaces; a small recirculation upstream Heater #1; the flow recirculation fulfills the entire cavity between Heaters #1 and #2, and also between Heaters #2 and #3; the detachment of the fluid's boundary layer at the top of the heater causing a recirculation (reverse flux); and a large recirculation region downstream Heater #3 due to the flow reattachment. The flow complexity around the array of 3D protruding heaters is greater with a larger *Re*.

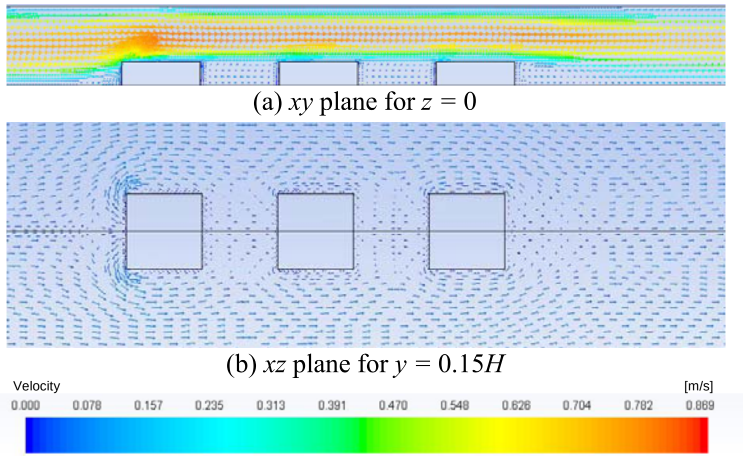

Figure 3. Velocity profile around an array of 3D protruding heaters for Re = 100.

3.2 Adiabatic substrate

In this case ($k_s/k = 0$) all the heat generation rate in each heater is transferred directly to the airflow by convection. Any active heater influences the temperature rise of all the others due to the flow recirculation induced by their protruding geometry, as described by Eq. (15) and shown in Fig. 3. The average *Nusselt* number for a single active heater in the array is presented in Fig. 4 and in Table 1 as a function of Re. Since these results were obtained for an adiabatic substrate, they indicate the adiabatic *Nusselt* number for each heater. They also reflect the thermal and flow development in the channel and a decrease of the heaters temperature with an increase of the channel flow rate. These results for each heater were correlated by a power law as in Eq. (14) with the coefficient C and the exponent m presented in Table 2.

$$\overline{Nu}_{0,n} = C\,Re^{m} \tag{14}$$

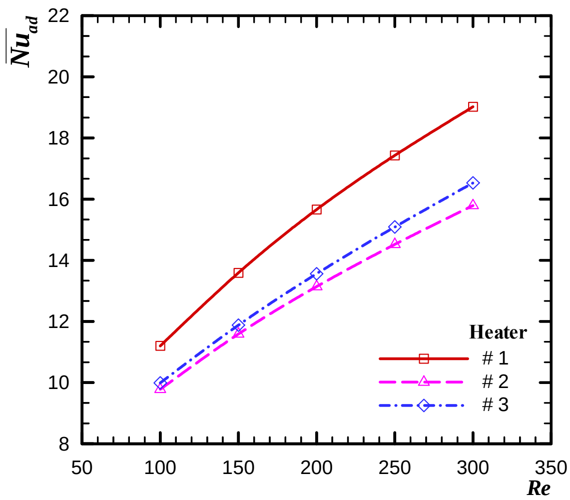

Figure 4. Average adiabatic *Nusselt* number for an adiabatic substrate and a single active heater.

Table 1. Average adiabatic *Nusselt* number for an adiabatic substrate and a single active heater.

Re	$Nu_{ad,1}$	$Nu_{ad,2}$	$Nu_{ad,3}$
100	11.20	9.78	9.99
150	13.59	11.59	11.88
200	15.66	13.14	13.56
250	17.43	14.52	15.09
300	19.02	15.79	16.53

Table 2. Coefficients of Eq. (14) for (k_s/k) = 0.

Heater	**#1**	**#2**	**#3**
C	1.2083	1.3095	1.2080
m	0.4833	0.4358	0.4575

Expressing the temperature difference by Eq. (8) for a 3D protruding heater

$$\Delta T_n = \left(T_h - T_0\right)_n = \frac{1}{\dot{m}\,c_p}\sum_{i=1}^{N} g_{ni}^{+}\left(\frac{q_i}{q_L}\right) \tag{15}$$

For a single active heater in the array, q_L in Eq. (15) indicates its heat dissipation rate. When the array has more than one active heater, q_L indicates the smallest heat generation rate of all the active heaters of the array. For a uniform heat generation rate in all the heaters, the ratio (q_i/q_L) is equal to one. The coefficients g_{ni}^{+} were obtained from numerical tests performed considering a single active heater in the array, replacing the heaters average surface temperature obtained from these tests in Eq. (15). With the same configuration and flow conditions, these coefficients are invariant with respect to the heaters dissipation rates. Thus, their average temperature may be obtained from Eq. (15) under any heating conditions of the array. For the adiabatic substrate this procedure is equivalent to that presented by Hacker & Eaton (1997) using the inverse discrete Green's function. For Re = 100, the coefficients of Eq. (15) were obtained numerically as follows

$$\begin{bmatrix} \Delta T_1 \\ \Delta T_2 \\ \Delta T_3 \end{bmatrix} = \frac{1}{\dot{m}\, c_p} \begin{bmatrix} g_{11}^{+} & g_{21}^{+} & g_{31}^{+} \\ g_{21}^{+} & g_{22}^{+} & g_{32}^{+} \\ g_{31}^{+} & g_{23}^{+} & g_{33}^{+} \end{bmatrix} \begin{bmatrix} q_1/q_L \\ q_2/q_L \\ q_3/q_L \end{bmatrix} = 2.3176 \begin{bmatrix} 67.1225 & 0.5834 & 0.0001 \\ 19.8808 & 76.8459 & 0.4866 \\ 12.2946 & 21.6663 & 75.1929 \end{bmatrix} \begin{bmatrix} q_1/q_L \\ q_2/q_L \\ q_3/q_L \end{bmatrix} \quad (16)$$

The diagonal terms of the influence coefficients matrix are associated to the self-heating of each heater. They are larger than the other terms, indicating that the heaters temperature rise is mostly influenced by their own heat generation rate. They increase slightly in the flow direction due to the thermal and flow development in the channel. The lower diagonal terms indicate for each heater the effects of the upstream heaters, caused mainly by the channel flow. They are larger than the upper diagonal terms, which represent the effects of the downstream heaters, caused by flow recirculation in the cavities between the heaters. The isotherm map (thermal wake) for Re = 100 is shown in Fig. 5.

Some predictions of Eq. (16) for the heaters' average temperatures under distinct dissipation rates in the array are presented in Table 3. The results for a single active heater are presented in the first three lines of Table 3. They may be superposed to obtain the heaters temperatures when the three heaters are active at the same time with arbitrary heat dissipation rates. Three examples are presented in the subsequent lines of Table 3. Test #4 considered the three heaters active with identical heat generation rates, 1W, indicated by the sequence (1-1-1). Tests #5 and #6 considered again all the heaters active, now with distinct heat generation rates proportional respectively to (0.4-0.3-0.3) and to (0.5-0.3-0.2). The results of the Tests #4 to #6 may be obtained either by superposition of the results from the Tests #1 to #3, or directly by Eq. (16). Numerical simulations were also performed under conditions identical to those of Tests #4 to #6, and the results were presented in Table 3 within 2%, a difference attributed to the truncation of the coefficients presented in Eq. (16).

Table 3. The temperature increase of each 3D protruding heater for Re =100 and (k_s/k) = 0.

Test	Active Heater	ΔT_1 [°C]	ΔT_2 [°C]	ΔT_3 [°C]
#1	**#1 (1-0-0)**	151.75	44.95	27.80
#2	**#2 (0-1-0)**	1.33	174.73	49.26
#3	**#3 (0-0-1)**	0.00	1.11	171.50
#4	**All (1-1-1)**	156.92	225.30	252.98
#5	**All (0.4-0.3-0.3)**	62.63	72.20	78.74
#6	**All (0.5-0.3-0.2)**	78.19	76.69	64.16

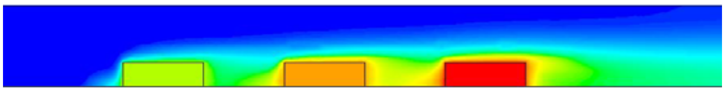
(a) xy plane for z = 0

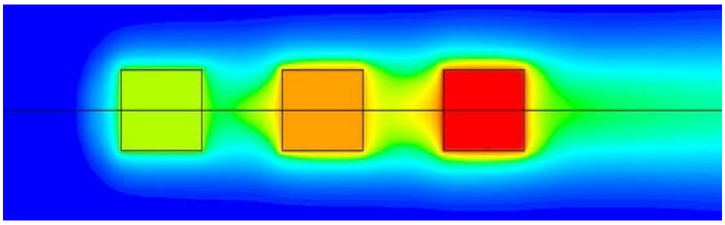
(b) xz plane for y = 0.15H

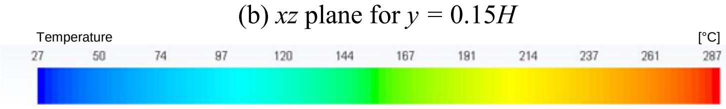

Figure 5. Isotherm maps for an adiabatic substrate and all heaters active (1-1-1).

3.3 Conductive substrate

For a conductive substrate, the heaters' cooling was simulated by a coupled forced convection-conduction mechanism. The substrate plate thickness was considered equal to 0.001m, with a thermal conductivity (k_s/k) equals to 84. The lower substrate surface was adiabatic, so that all the heat conducted from the heaters eventually returned to the flow by convection both upstream and downstream of each heater. For example, when only Heater #2 was active, the results for the fraction (q_{cd}/q) of the power transferred by conduction are presented in Fig. 6. They show that the conductive fraction decreases with *Reynolds* number. The observed decrease is due mainly to a larger flow velocity over the heaters' surfaces, increasing the convection from the heaters. These results showed that the conduction from the heaters may not be neglected and that it depends strongly on the substrate thermal conductivity. Results obtained for the other two heaters presented quite similar trends, indicating thus the important role played by a conductive substrate on the thermal control of electronic components.

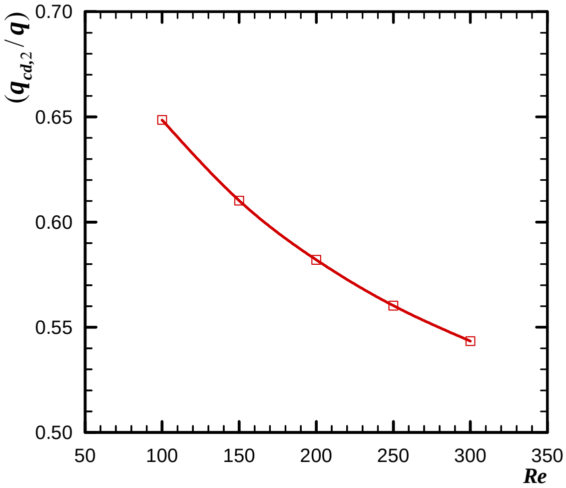

Figure 6. Conduction fraction (q_{cd}/q) for only Heater #2 active.

The heaters average temperatures in the case of conjugate forced convection-conduction cooling may also be obtained from Eq. (15). The conjugate influence coefficients g_{ni}^{+} were obtained in this case by a procedure similar to that for the adiabatic substrate, but now considering a finite substrate thermal conductivity. Repeating the condition of Re = 100, the conjugate coefficients for (k_s/k) = 84 are indicated in Eq. (17).

$$\begin{bmatrix} \Delta T_1 \\ \Delta T_2 \\ \Delta T_3 \end{bmatrix} = \frac{1}{\dot{m}c_p} \begin{bmatrix} g_{11}^{+} & g_{21}^{+} & g_{31}^{+} \\ g_{21}^{+} & g_{22}^{+} & g_{32}^{+} \\ g_{31}^{+} & g_{23}^{+} & g_{33}^{+} \end{bmatrix} \begin{bmatrix} q_1/q_L \\ q_2/q_L \\ q_3/q_L \end{bmatrix} = 2.3176 \begin{bmatrix} 27.0295 & 3.9843 & 0.5866 \\ 9.7112 & 28.6385 & 4.1694 \\ 5.7867 & 10.1041 & 28.7957 \end{bmatrix} \begin{bmatrix} q_1/q_L \\ q_2/q_L \\ q_3/q_L \end{bmatrix} \tag{17}$$

In this case also, the largest terms in Eq. (17) are the diagonal coefficients, corresponding to self-heating, and they increase slightly downstream, as in the previous case. Due to the conjugate cooling of the heaters array, they are however smaller than the diagonal terms of Eq. (16). The lower diagonal terms in Eq. (17) are only slightly larger than the corresponding terms in Eq. (16), since they represent the effects of the upstream heaters, influenced mostly by the channel flow. On the other hand, the upper diagonal terms in Eq. (17) are noticeably larger than the corresponding values in Eq. (16) because now the influence of the downstream heaters is enhanced by conduction in the substrate. The isotherm map (thermal wake) for Re = 100 is shown in Fig. 7.

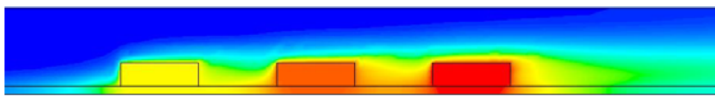

(a) xy plane for z = 0

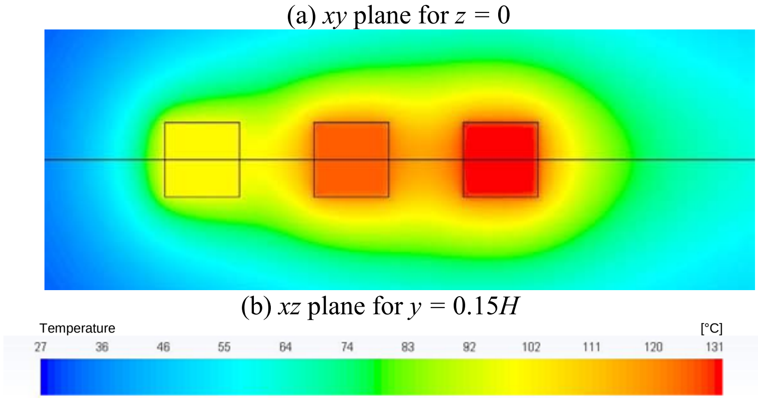

(b) xz plane for y = 0.15H

Figure 7. Isotherm maps for a conductive substrate and all heaters active (1-1-1).

Considering the same power dissipation in the array, the heaters' temperature predicted by Eq. (17) for the conductive substrate will be more uniform than the predictions of Eq. (16) for the adiabatic substrate. This can be seen in Table 4, obtained from numerical tests performed for a conductive substrate with (k_s/k) = 84 under conditions analogous to those presented in Table 3. For the first three tests, with a single active heater at a time, the active heater temperature is lower for the conductive substrate than for the adiabatic substrate. On the other hand, in each of these tests, the temperatures of the two unpowered heaters are comparatively slightly higher due to conduction in the substrate. The remaining three tests, performed with the three heaters active, indicate that their temperatures are lower than the corresponding values for the adiabatic substrate, as was presented in Table 3. These results indicate the relevance of the conductive substrate in the cooling of electronic components.

Table 4. The temperature increase of each 3D protruding heater for *Re* =100 and (k_s/k) = 84

Test	Active Heater	ΔT_1 [°C]	ΔT_2 [°C]	ΔT_3 [°C]
#1	**#1 (1-0-0)**	62.60	22.49	13.40
#2	**#2 (0-1-0)**	9.23	66.33	23.40
#3	**#3 (0-0-1)**	1.35	9.62	66.47
#4	**All (1-1-1)**	73.24	98.54	103.57
#5	**All (0.4-0.3-0.3)**	28.24	31.81	32.41
#6	**All (0.5-0.3-0.2)**	34.36	33.10	27.08

4. CONCLUSIONS

The quest for invariant descriptors of heat transfer process with non-uniform thermal boundary conditions (for the same geometry, fluid flow and physic properties) was the challenge of this work. In the available literature, two invariant descriptors of convective heat transfer process were found. The first one was the adiabatic heat transfer coefficient based on the adiabatic surface temperature and the other was the treatment by discrete Green's function. In this work, a square matrix G^+ with conjugate influence coefficients g^+ was numerically validated as invariant descriptor of conjugate forced convection-conduction heat transfer. The described procedure is however general and extensions to larger number of heaters are straightforward, although computationally more demanding.

5. ACKNOWLEDGEMENTS

The authors thank the National Council for Scientific and Technological Development (CNPq), a foundation linked to the Ministry of Science and Technology and Innovation (MCTI), as well as the Federal University of Technology – Paraná (UTFPR) for the financial support.

6. REFERENCES

Alves, T.A. and Altemani, C.A.C., 2012. "An invariant descriptor for heaters temperature prediction in conjugate cooling". *Int. J. Th. Sc.*, Vol. 58, pp. 92–101.

Anderson, A.M. and Moffat, R.J., 1992a. "The adiabatic heat transfer coefficient and the superposition kernel function: part 1 – data for arrays of flatpacks for different flow conditions". *J. Electron. Packag.*, Vol. 114, pp.14-21.

Anderson, A.M., 1994. "Decoupling convective and conductive heat transfer using the adiabatic heat transfer coefficient". *J. Electron. Packag.*, Vol. 116, pp. 310-316.

Anderson, A.M. and Moffat, R.J., 1992b. "The adiabatic heat transfer coefficient and the superposition kernel function: part 2 – modeling flatpack data as a function of channel turbulence". *J. Electron. Packag.*, Vol. 114 pp. 22-28.

ANSYS/Fluent^{TM}, 2011. "Tutorial, 2011: solving a conjugate heat transfer problem using ANSYS/Fluent^{TM}". pp. 1-30.

Arvizu, D.E. and Moffat, R.J., 1982. "The use of superposition in calculating cooling requirements for circuit-board-mounted electronic components". *Proc. of 32nd Elect. Cool. Conf.*, pp.133–144.

Bar-Cohen, A., Watwe, A.A. and Prasher, R.S., 2003 "Heat Transfer in Electronic Equipment." In Bejan, A. and Kraus, A. D., Eds., *Heat Transfer Handbook*, John Wiley & Sons., New Jersey, USA, pp.947-1027.

Bergman, L., Lavine, A.S., Incropera, F.P. and Dewitt, D.P., 2012. *Fundamentals of heat and mass transfer*. John Wiley & Sons., New Jersey, USA.

Davalath, J. and Bayazitoglu, Y., 1987. "Forced convection cooling across rectangular blocks". *J. Heat Transf.*, Vol. 109, pp. 321-328.

Eckert, E.R.G. and Drake, R.M., 1972. *Analysis of Heat and Mass Transfer*. McGraw-Hill, New York, USA.

Hacker, J.M. and Eaton, J.K., 1997. "Measurements of heat transfer in separated and reattaching flow with spatially varying thermal boundary conditions". *Int. J. Heat Fluid Flow*, Vol. 18, pp. 131-141.

Moffat, R.J., 1998. "What's new in convective heat transfer?". *Int. J. Heat Fluid Flow*, Vol. 19, pp. 90-101.

Moffat, R.J., 2004. "$h_{adiabatic}$ and u'_{max}". *J. Electron. Packag.*, Vol. 126, pp. 501-509.

Moffat, R.J. and Anderson, A.M., 1990. "Applying heat transfer coefficient data to electronics cooling". *J. Heat Transf.*, Vol. 112, pp. 882-890.

Patankar, V., 1980. *Numerical heat transfer and fluid flow*. Hemisphere Publishing Corporation, New York, USA.

Zeng, Y. and Vafai, K., 2009. "An investigation of convective cooling of an array of channel-mounted obstacles". *Num. H. Transf.*, Vol. 55, pp. 967-982.

7. RESPONSIBILITY NOTICE

The authors are the only responsible for the printed material included in this paper.